

Electronic supplementary information (ESI)

How Uniform Particle Size of NMC90 Boosts Li-ion Mobility for Faster Charging and Discharging at a Cylindrical Li-ion Battery Cell

Nichakarn Anansuksawat, Thitiphum Sangsanit, Surat Prempluem, Kan Homlamai, Worapol Tejangkura, and Montree Sawangphruk*

Centre of Excellence for Energy Storage Technology (CEST), Department of Chemical and Biomolecular Engineering, School of Energy Science and Engineering, Vidyasirimedhi Institute of Science and Technology, Rayong 21210, Thailand

Supporting results

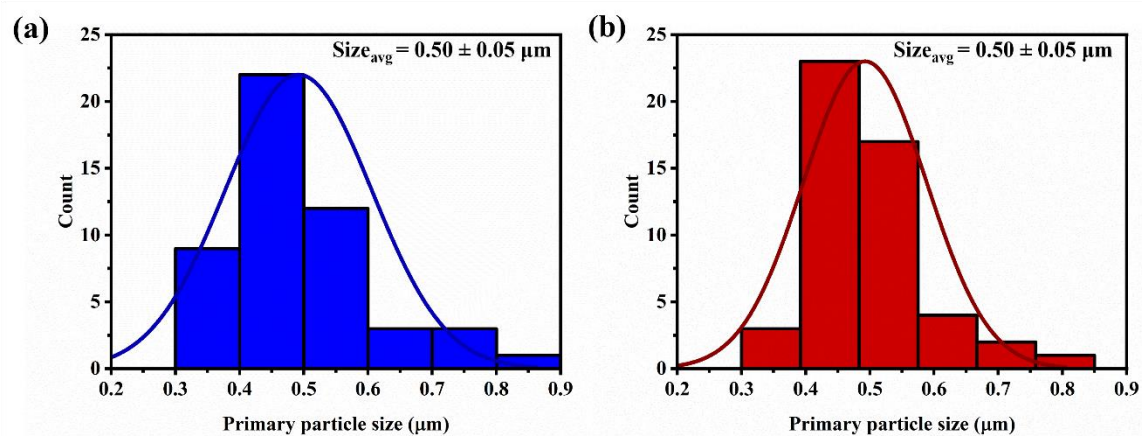


Fig. S1. primary particle size distribution of (a) NMC90 powder and (b) NMC80 powder.

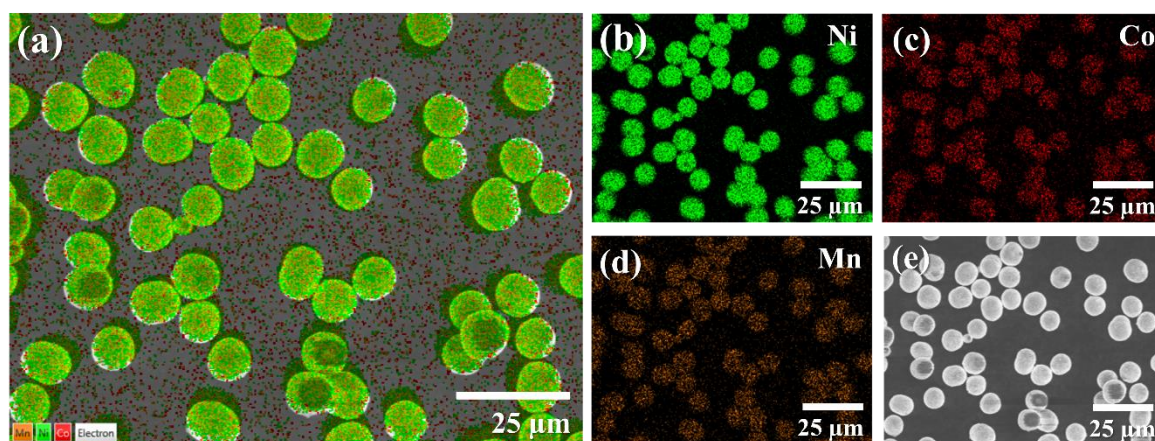


Fig. S2. SEM-EDX element mapping images of NMC90 powder: (a) all overlaying elements, (b) Ni, (c) Co, and (d) Mn, and FESEM image of (e) NMC90 powder at top view.

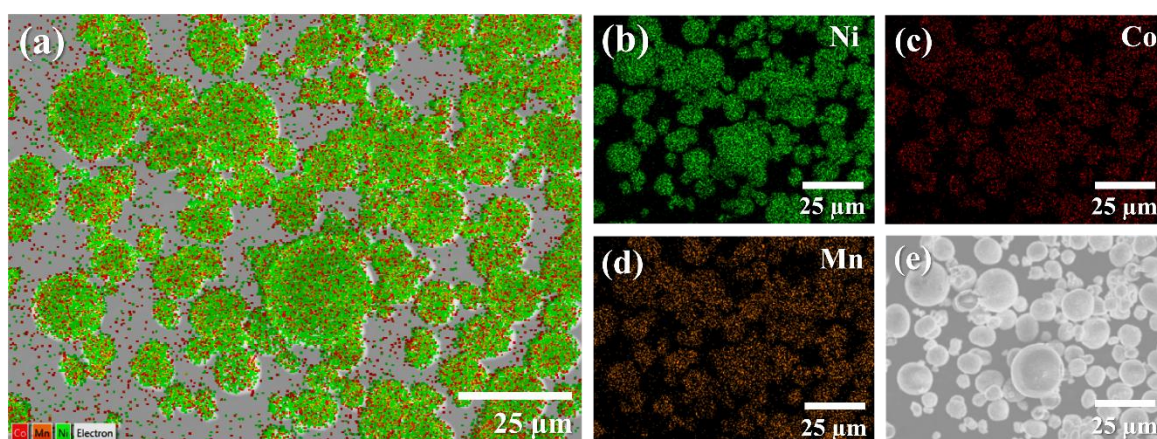


Fig. S3. SEM-EDX element mapping images of NMC80 powder: (a) all overlaying elements, (b) Ni, (c) Co, and (d) Mn, and FESEM image of (e) NMC80 powder at top view.

Table S1. Elemental composition of NMC80 and NMC90 powders.

Element	Elemental composition (Wt. %)	
	NMC80 powder	NCM90 powder
Ni	80.3	90.1
Co	10.7	5.2
Mn	9.0	4.7

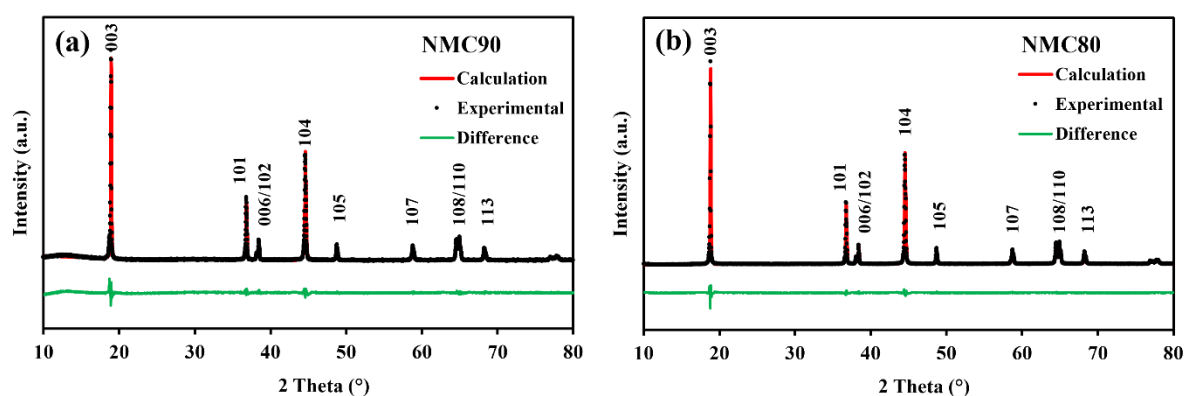


Fig. S4. Rietveld refinement of (a) NMC90 powder and (b) NMC80 powder.

Table S2. Rietveld refinement results of XRD patterns of NMC80 and NMC90 powder.

Parameters	NMC80	NMC90
Lattice constant a (Å)	2.8722(0)	2.8751(0)
Lattice constant c (Å)	14.2051(0)	14.2029(0)
V (Å ³)	101.4855(7)	101.6748(6)
n Ni in Li sites	1.78%	1.24%
R _B	0.75	1.30
R _{wp}	2.05	2.74

Table S3. BET surface area, pore volume, and pore size of NMC80 and NMC90 electrodes.

Sample	BET		
	Surface area (m ² /g)	Pore volume (cm ³ /g)	Pore size (nm)
NMC80 powder	0.2876	0.001082	8.8497
NMC90 powder	0.2678	0.001195	9.3782
NMC80 electrode	1.0883	0.003249	11.9419
NMC90 electrode	1.0347	0.002563	9.9088

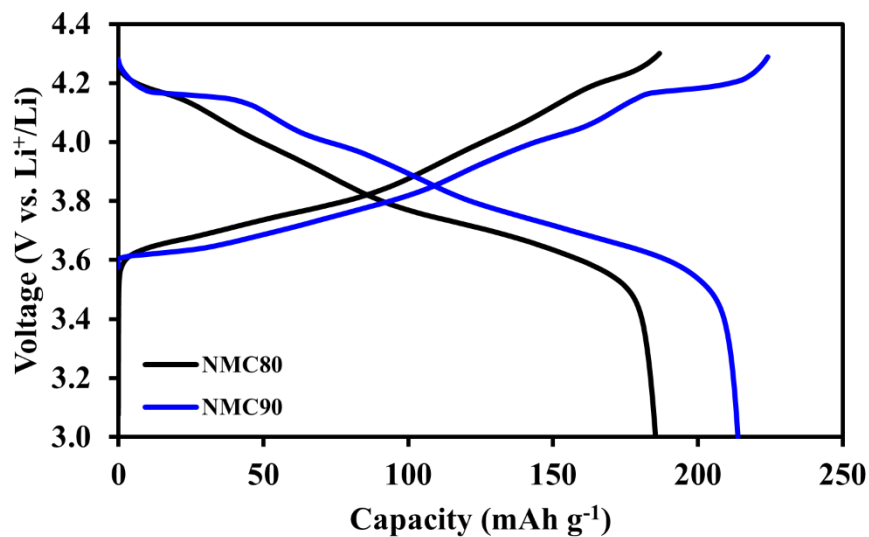


Fig. S5. Voltage profiles in half-cell coin cell configuration at 0.1C within the voltage range of 3.0-4.3 V of NMC90 (red line) and NMC80 (black line).

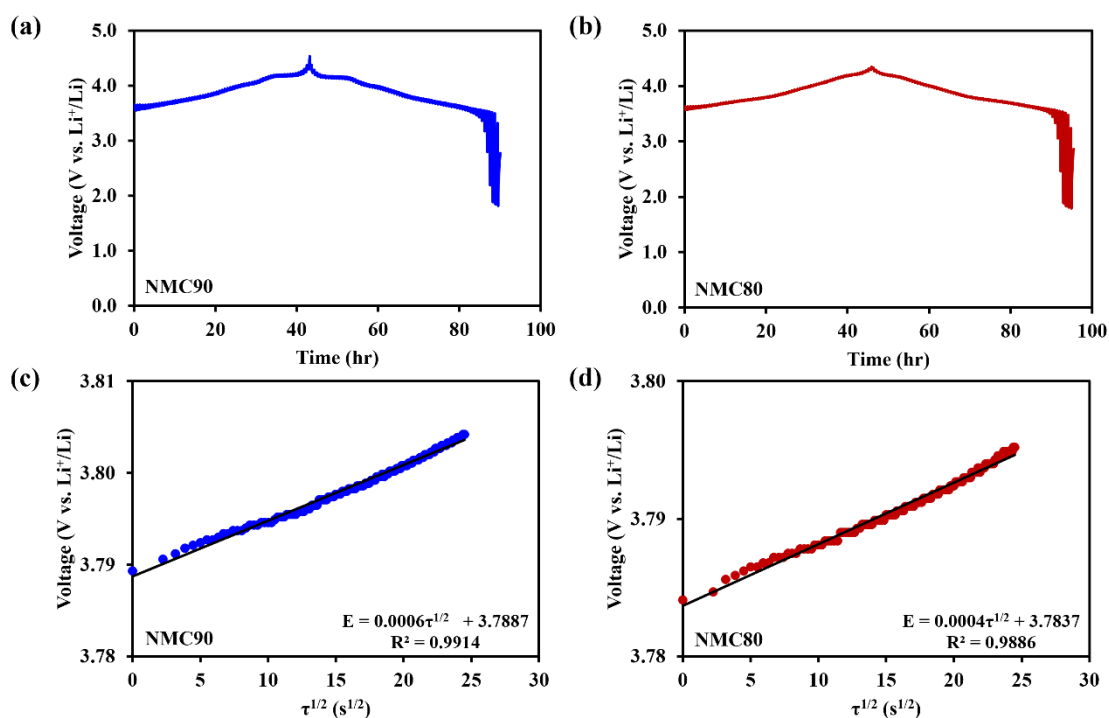


Fig. S6. Galvanostatic intermittent titration technique (GITT) curves vs. time of (a) NMC90 and (b) NMC80, the relationship of the cell voltage and $\tau^{1/2}$ for the titration curves of (c) NMC90 and (d) NMC80.

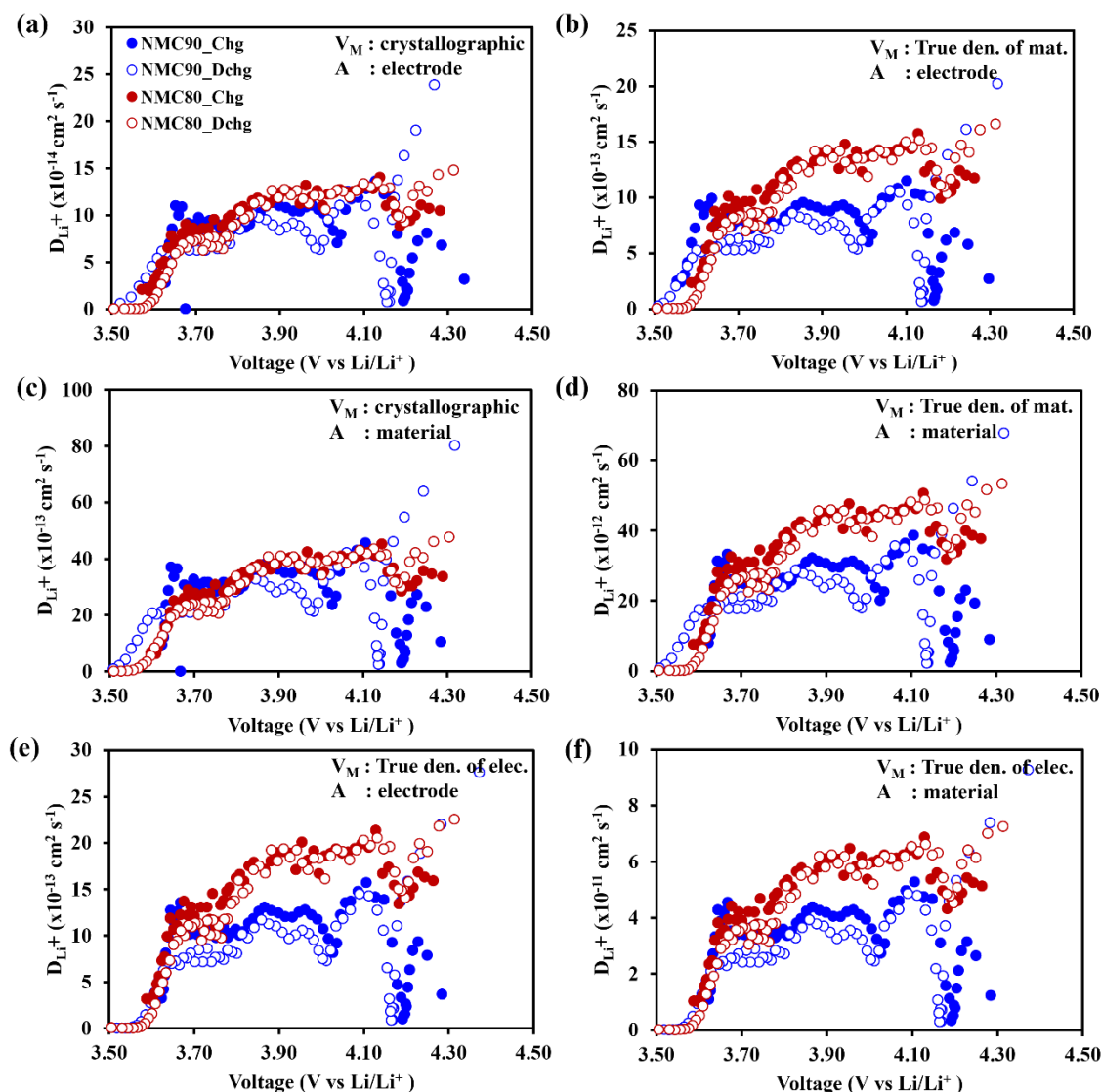


Fig. S7. The lithium diffusivity from GITT measurement of NMC90 and NMC80 during charging and discharging as a function of the cell potential with various setting parameters of V_M and A : (a) V_M from crystallographic and A from surface area of the electrode, (b) V_M from true density of the active material and A from surface area of the electrode, (c) V_M from crystallographic and A from surface area of the active material, (d) V_M from true density of the active material and A from surface area of the active material, (e) V_M from true density of the electrode and A from surface area of the electrode, and (f) V_M from true density of the electrode and A from surface area of the active material.

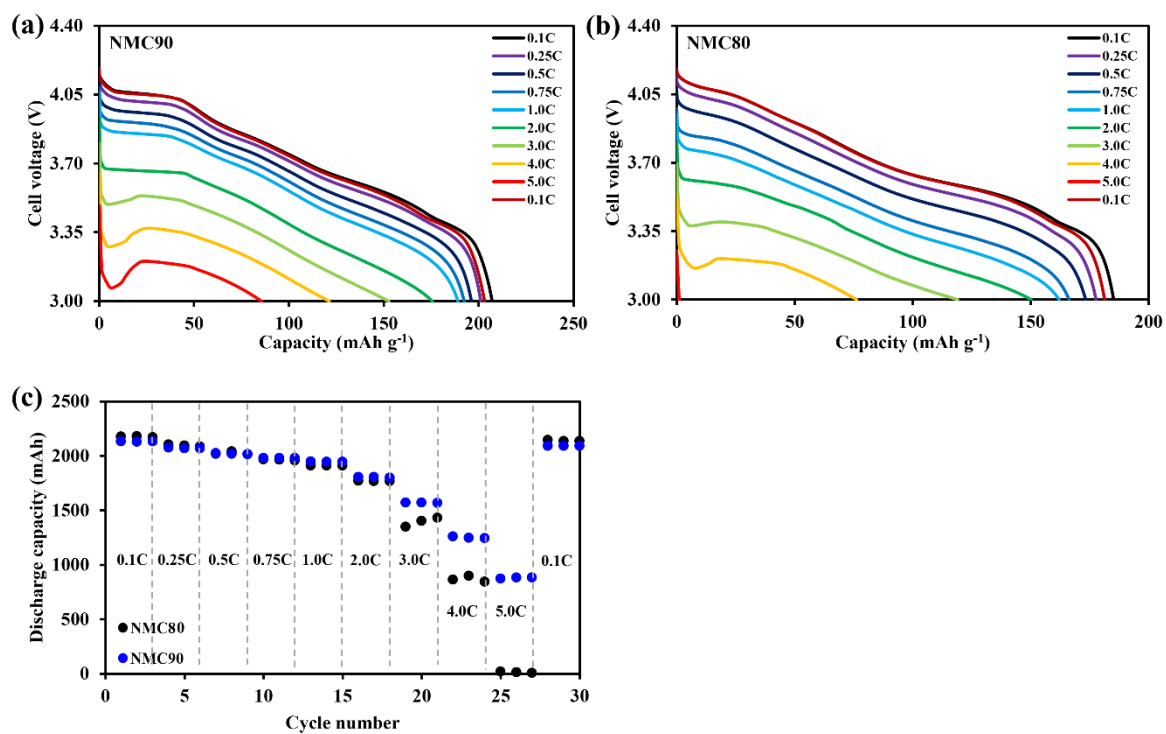


Fig. S8. Rate capability in cylindrical configuration at various current density from 0.1C to 5.0C within the voltage range of 3.0-4.2 V: voltage profiles at each C-rate of (a) NMC90 and (b) NMC80, and (c) discharge capacity based on cell.

Table S4. IR drop from rate capability at various current density from 0.1C to 5.0C within the voltage range of 3.0-4.2 V of NMC90 and NMC80 cells.

C-rate	IR drop (V)	
	NMC90	NMC80
0.1C	0.0191	0.0284
0.25C	0.0377	0.0631
0.5C	0.0746	0.1196
0.75C	0.1152	0.1937
1.0C	0.1348	0.2572
2.0C	0.2743	0.3908
3.0C	0.3986	0.5055
4.0C	0.5474	0.6640
5.0C	0.7151	0.9495
0.1C	0.0185	0.0213

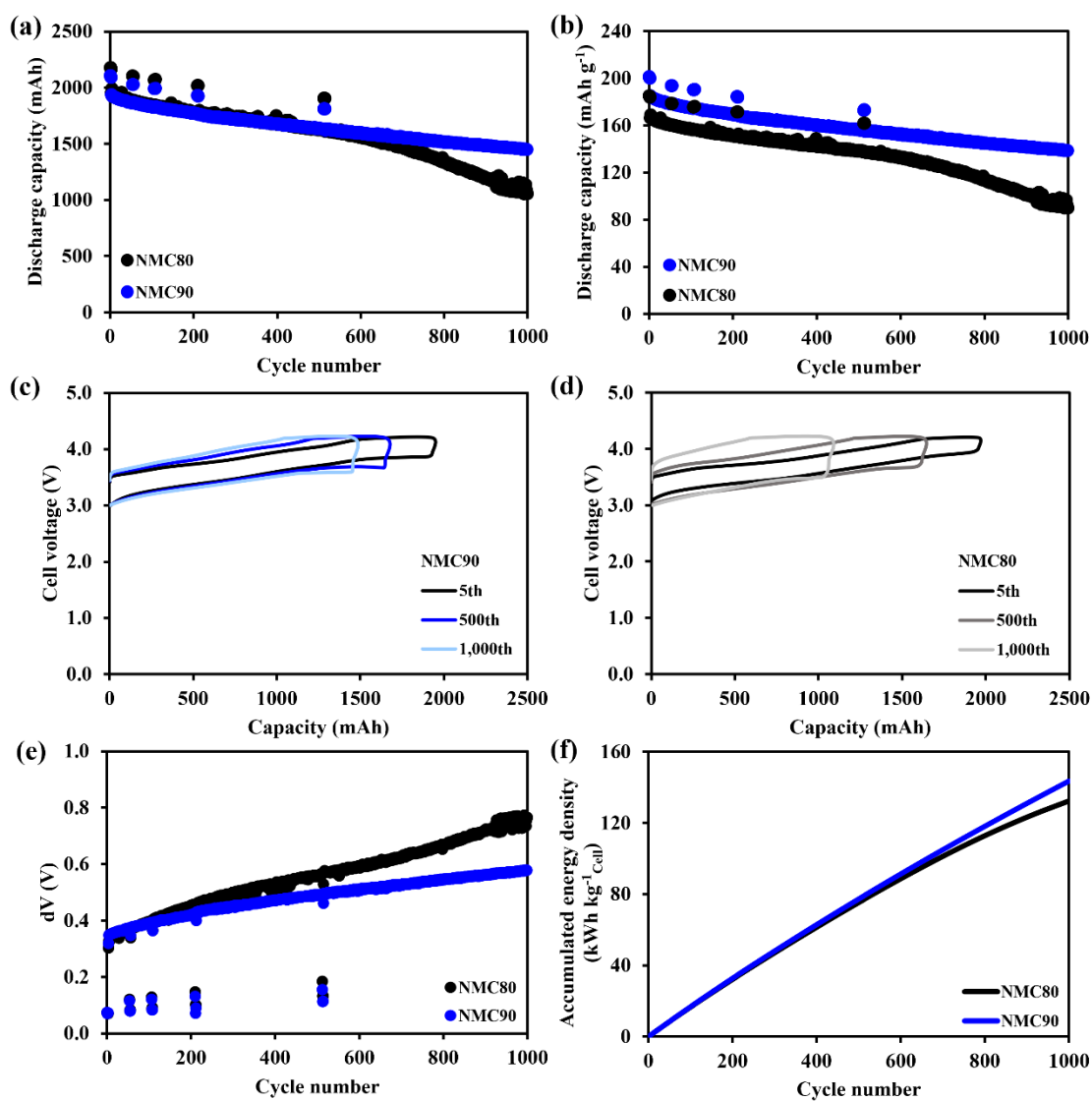


Fig. S9. Long-term cycling performance with the window potential of 3.0-4.2V at 0.5C CCCV-charge and 1.0C CC-discharge: discharge capacity based on (a) cell and (b) active cathode material, voltage profiles of (c) NMC90 and (d) NMC80, (e) voltage differential of charge and discharge curves, and (f) accumulated energy density based on the cell level.

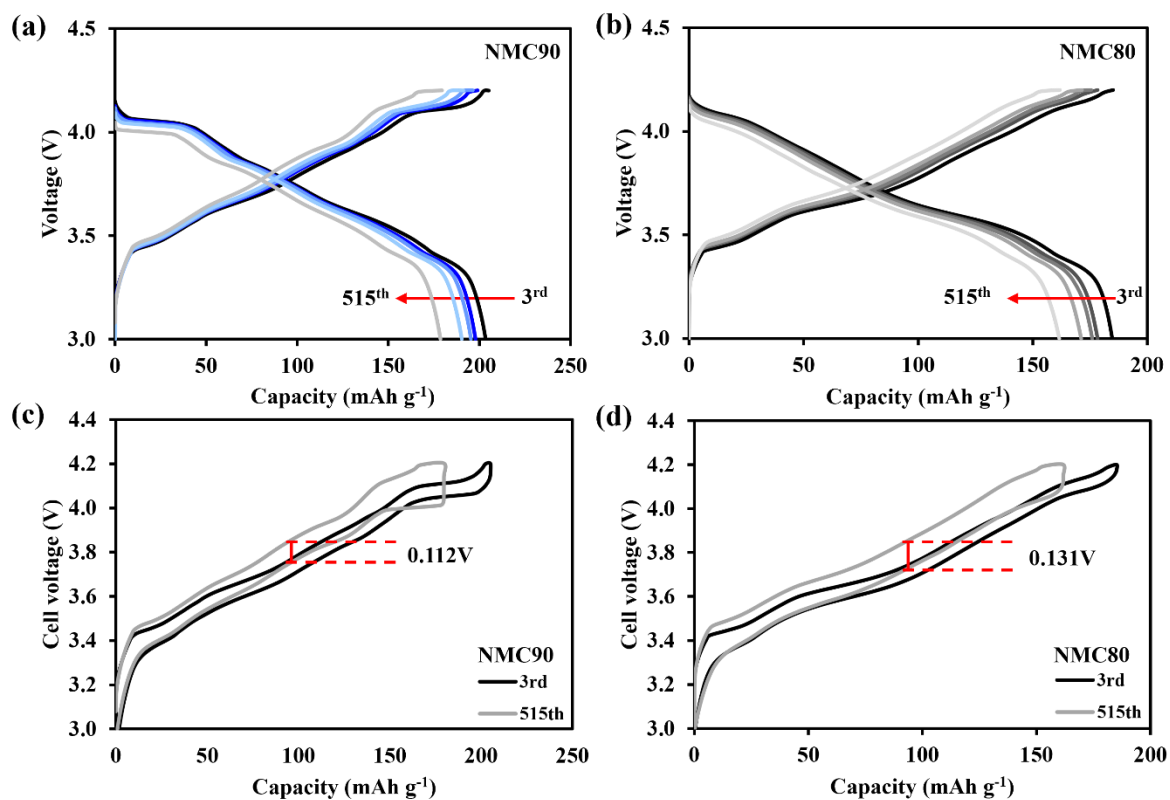


Fig. S10. Voltage profiles at check-up step (0.1C) for long-term cycling with cycle numbers of the 3rd, 56th, 109th, 212th, and 515th cycles of (a, c) NMC90 and (b, d) NMC80.

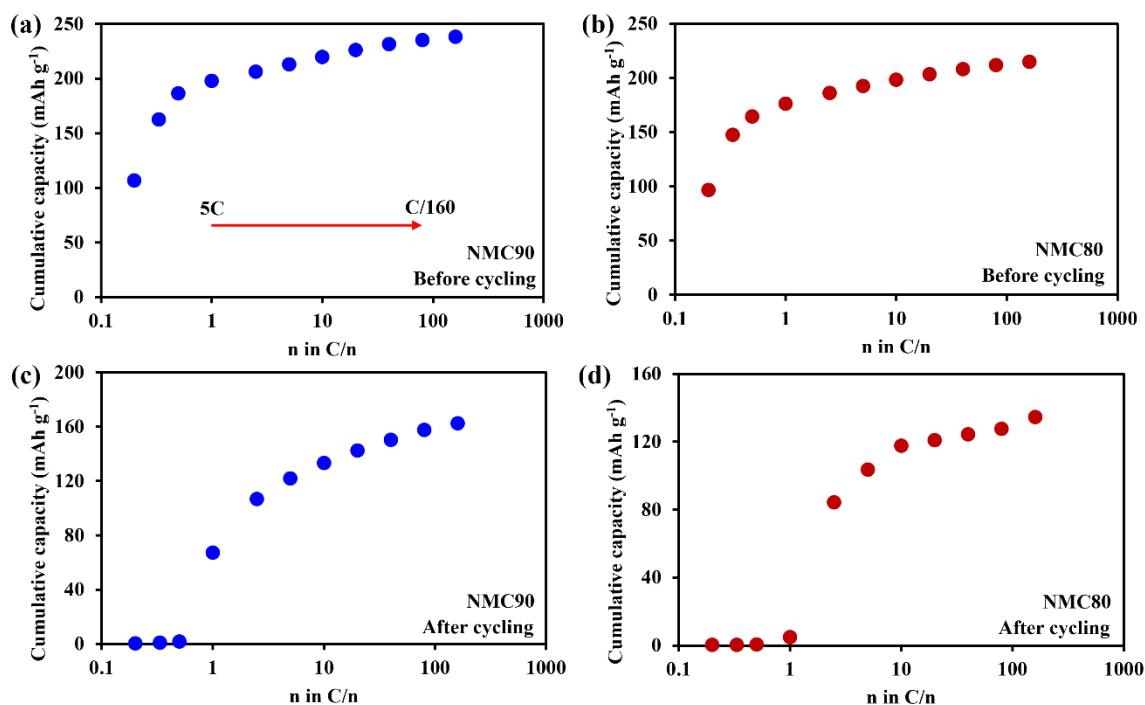


Fig. S11. The cumulative capacities obtained from the Atlung Method for Intercalant Diffusion (AMID) before cycling of (a) NMC90 and (b) NMC80 and after cycling of (c) NMC90 and (d) NMC80 for 3.0-4.3 V with C-rates from 5C to C/160 in half-cell coin cell configuration.

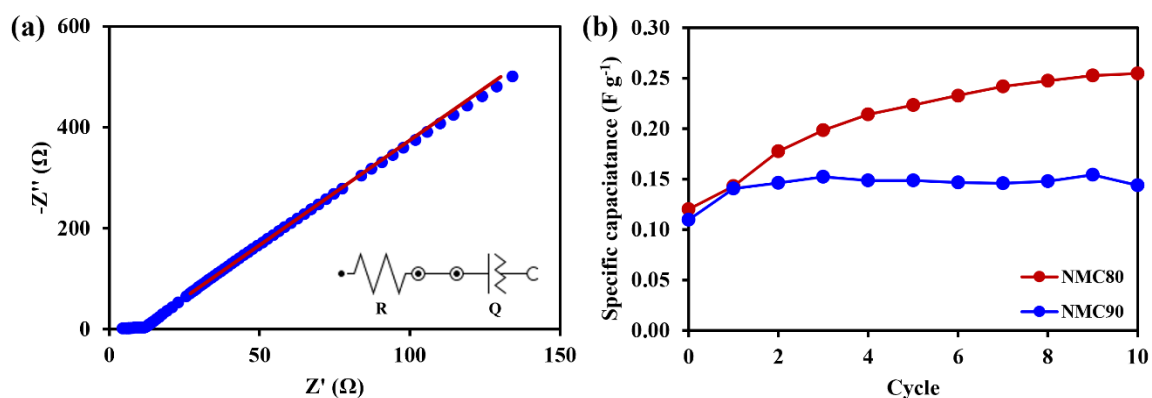


Fig. S12. (a) example of the Nyquist plot with equivalent circuit for capacitance measurement (blue dot is impedance data and red line is EIS fitting curve) and (b) specific capacitance of NMC80 and NMC90 cells for 10 cycles.

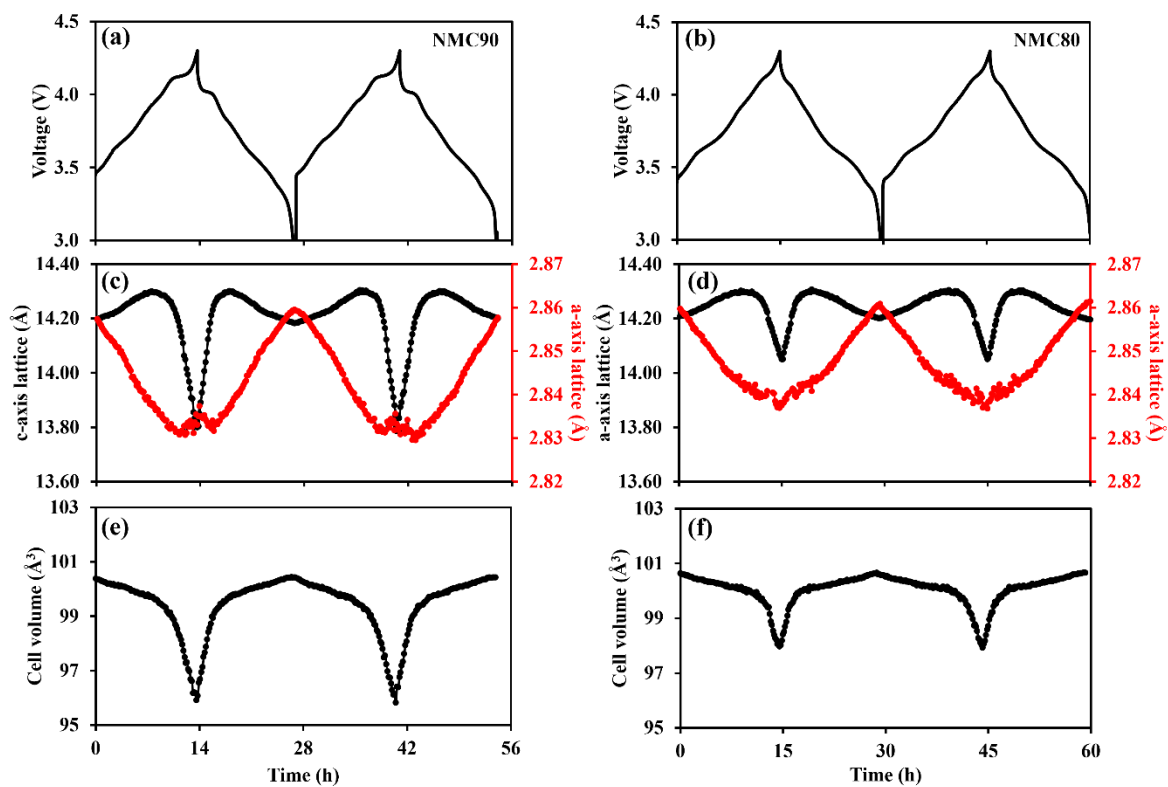


Fig. S13. The structural change from refinement results for (left) NMC90-graphite and (right) NMC80-graphite were operated in pouch cells. (a, b) voltage profiles, (c, d) lattice parameter a and c, and (e, f) unit cell volume for 2 cycles.

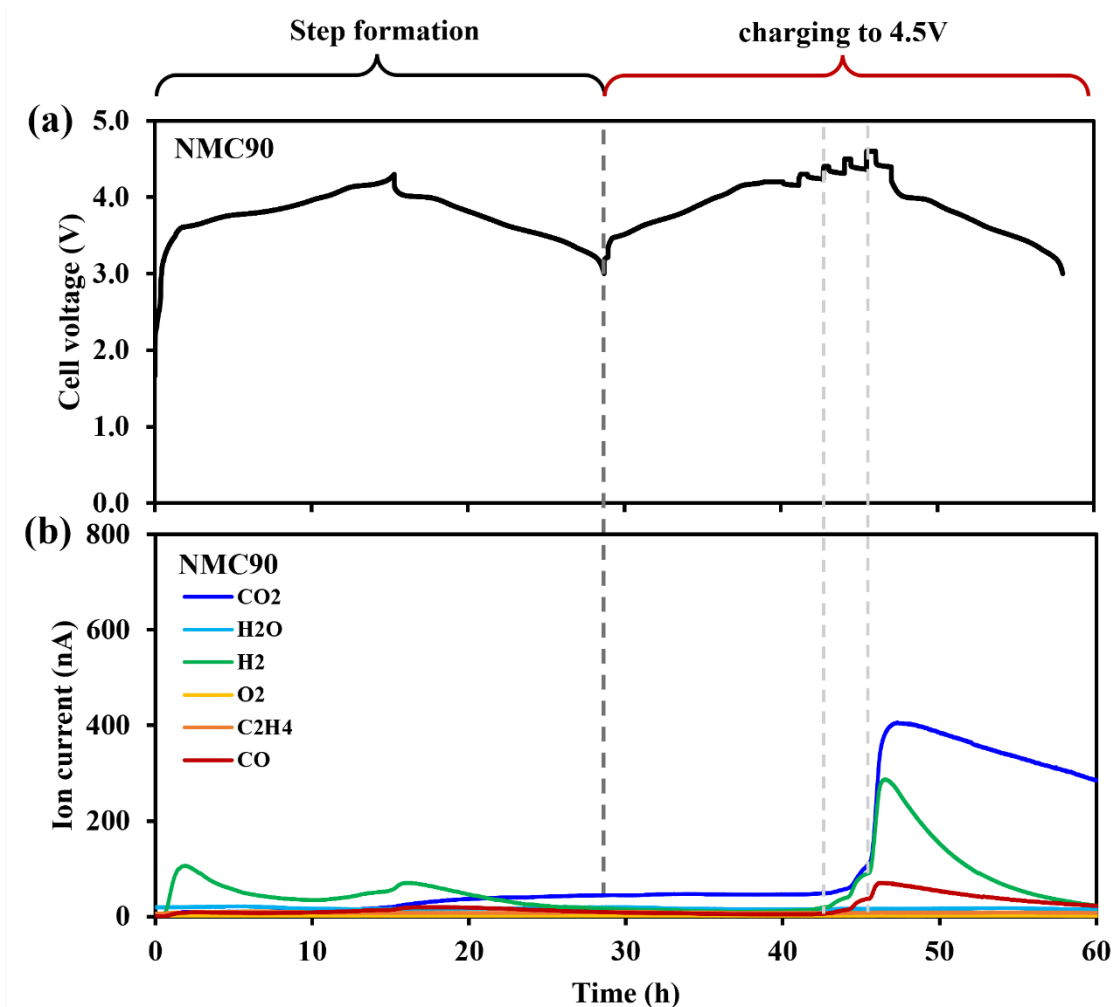


Fig. S14. (a) the voltage profile of NMC90-graphite cell during the step formation and the first cycle with the upper cutoff voltage of 4.5V in 18650 cylindrical configuration and (b) the corresponding gas evolution as a function of time of NMC90-graphite cell detected by *in situ* DEMS measurement.

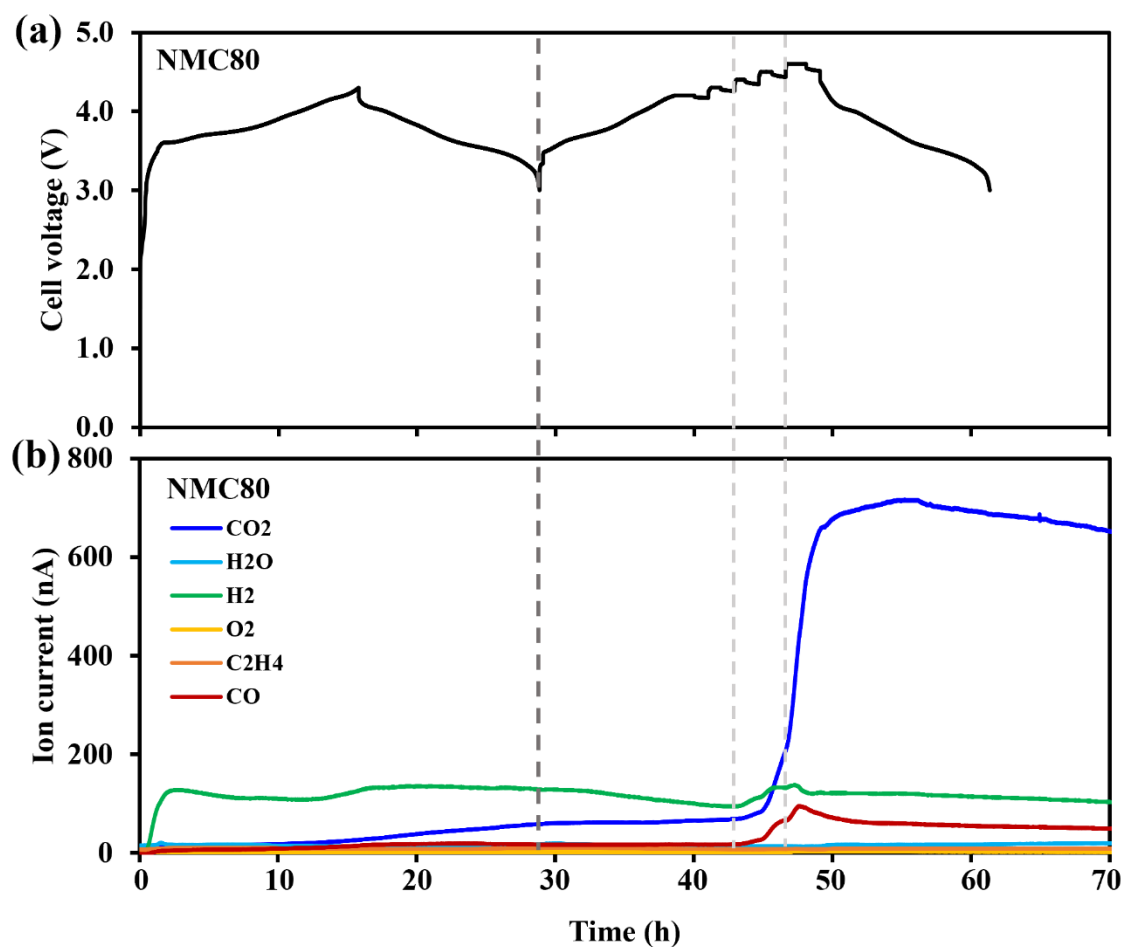


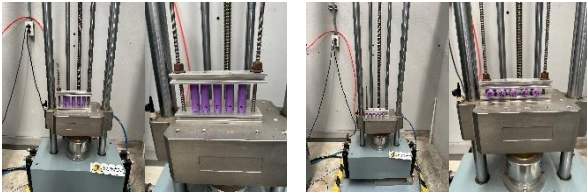




Fig. S15. (a) the voltage profile of NMC80-graphite cell during the step formation and the first cycle with the upper cutoff voltage of 4.6V in 18650 cylindrical configuration and (b) the corresponding gas evolution as a function of time of NMC80-graphite cell detected by *in situ* DEMS measurement.

Table S5. Summary results of NMC80 and NMC90 after evaluating the safety test

Test name	Passing rate (%)	
	NMC80	NMC90
Altitude test	100	100
		
Thermal test	100	100
		
Shock test	100	100
		
Short circuit test	100	100
		
Impact test	100	100
		

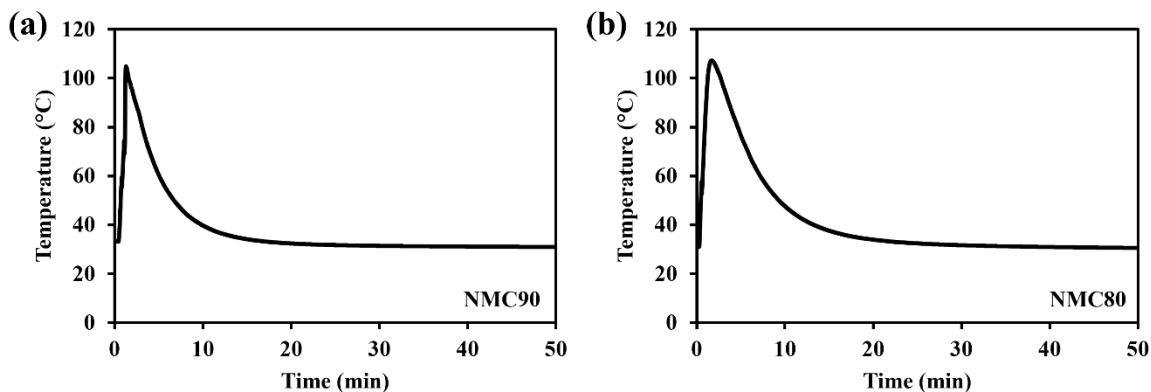


Fig. S16. Temperature profiles from impact test following UN38.3 standard of (a) NMC90 and (b) NMC80.

Links to supporting VDOs

1. Thermal test of NMC80 and NMC90 18650 Li-ion batteries

<https://vistec->

my.sharepoint.com/:v:/g/person/nichakarn_a_s19_vistec_ac_th/EXQUpr4p4KZMk

[FJePFyUyUcBHm6OAVOTX6AVsoFELC72iQ?e=FAfQ9A](https://my.sharepoint.com/:v:/g/person/nichakarn_a_s19_vistec_ac_th/EXQUpr4p4KZMkFJePFyUyUcBHm6OAVOTX6AVsoFELC72iQ?e=FAfQ9A)

2. Shock test of NMC80 and NMC90 18650 Li-ion batteries

<https://vistec->

my.sharepoint.com/:v:/g/person/nichakarn_a_s19_vistec_ac_th/ETPJAo1bAY9Euv

[SwRWu0aVMBMy9nzciPmhKd3sv8VnMhcA?e=ebc7gc](https://my.sharepoint.com/:v:/g/person/nichakarn_a_s19_vistec_ac_th/ETPJAo1bAY9EuvSwRWu0aVMBMy9nzciPmhKd3sv8VnMhcA?e=ebc7gc)

3. Impact test of NMC80 and NMC90 18650 Li-ion batteries

<https://vistec->

my.sharepoint.com/:v:/g/person/nichakarn_a_s19_vistec_ac_th/EbloCH41mWJOqG

[OhRKLrVFQBaxz9-1Wuwco2cFCos8_vTA?e=89e0ZW](https://my.sharepoint.com/:v:/g/person/nichakarn_a_s19_vistec_ac_th/EbloCH41mWJOqGOhRKLrVFQBaxz9-1Wuwco2cFCos8_vTA?e=89e0ZW)